GEOLOGY

E: geology@geosociety.org
W: geosociety.org/gsa
T: @geosociety

FOR PEER REVIEW - CONFIDENTIAL

Early onset and late acceleration of rapid exhumation in the Namche Barwa syntaxis, eastern Himalaya

Tracking no: G47720R

Authors:
Gwladys Govin (Lancaster University), Peter van der Beek (Universite Grenoble Alpes), Yani Najman (Lancaster University), Ian Millar (NERC Isotope Geoscience Laboratories), Lorenzo Gemignani (Freie Universitaet Berlin), Pascale Huyghe (Universite Grenoble Alpes), Guillaume Dupont Nivet (CNRS - University of Potsdam), Matthias Bernet (Universite Grenoble Alpes), Chris Mark (University College Dublin), and Jan Wijbrans (Vrije Universiteit Amsterdam)

Abstract:
The Himalayan syntaxes, characterized by extreme rates of rock exhumation co-located with major trans-orogenic rivers, figure prominently in the debate on tectonic versus erosional forcing of exhumation. Both the mechanism and timing of rapid exhumation of the Namche Barwa massif in the eastern syntaxis remain controversial. It has been argued that coupling between crustal rock advection and surface erosion initiated in the late Miocene (8-10 Ma). Recent studies, in contrast, suggest a Quaternary onset of rapid exhumation linked to a purely tectonic mechanism. We report new multisystem detrital thermochronology data from the most proximal Neogene clastic sediments downstream of Namche Barwa and use a thermo-kinematic model constrained by new and published data to explore its exhumation history. Modeling results show that exhumation accelerated to ~4 km/m.y. at ~8 Ma and to ~9 km/m.y. after ~2 Ma. This three-stage history reconciles apparently contradictory evidence for early and late onset of rapid exhumation, and suggests efficient coupling between tectonics and erosion since the late Miocene. Quaternary acceleration of exhumation is consistent with river-profile evolution, and may be linked to a Quaternary river-capture event.

Early onset and late acceleration of rapid exhumation in the Namche Barwa syntaxis, eastern Himalaya

Gwladys Govin[1†], Peter van der Beek[2,3*], Yani Najman[1], Ian Millar[4], Lorenzo Gemignani[5‡], Pascale Huyghe[2], Guillaume Dupont-Nivet[3,6], Matthias Bernet[2], Chris Mark[7§], Jan Wijbrans[5]

[1] Lancaster Environment Centre, Lancaster University, Lancaster, UK.

[2] Université Grenoble Alpes, Institut des Sciences de la Terre (ISTerre), Grenoble, France.

[3] Department of Geosciences, Potsdam University, Potsdam, Germany.

[4] NERC Isotope Geosciences Laboratory, British Geological Survey, Keyworth, UK.

[5] VU University, Department of Earth Sciences, Amsterdam, the Netherlands.

[6] CNRS, Univ. Rennes 1, Géosciences Rennes, Rennes, France.

[7] Department of Geology, Trinity College Dublin, Dublin, Ireland.

† Deceased.

* Corresponding author: Peter van der Beek (vanderbeek@uni-potsdam.de).

‡ Now at: Institute of Geological Sciences, Freie Universität Berlin, Berlin, Germany.

§ Now at: School of Earth Sciences, University College Dublin, Dublin, Ireland.

ABSTRACT

The Himalayan syntaxes, characterized by extreme rates of rock exhumation co-located with major trans-orogenic rivers, figure prominently in the debate on tectonic versus erosional forcing of exhumation. Both the mechanism and timing of rapid exhumation of the Namche Barwa massif in the eastern syntaxis remain controversial. It has been argued that coupling between crustal rock advection and surface erosion initiated in the late Miocene (8-10 Ma). Recent studies, in contrast, suggest a Quaternary onset of rapid exhumation linked to a purely tectonic mechanism. We report new multisystem detrital thermochronology data from the most proximal Neogene clastic sediments downstream of Namche Barwa and use a thermo-kinematic model constrained by new and published data to explore its exhumation history. Modeling results show that exhumation accelerated to ~4 km/m.y. at ~8 Ma and to ~9 km/m.y. after ~2 Ma. This three-stage history reconciles apparently contradictory evidence for early and late onset of rapid exhumation, and suggests efficient coupling between tectonics and erosion since the late Miocene. Quaternary acceleration of exhumation is consistent with river-profile evolution, and may be linked to a Quaternary river-capture event.

INTRODUCTION

The Nanga Parbat and Namche Barwa massifs, at the respective western and eastern syntaxial terminations of the Himalaya (Fig. 1) share characteristics that have focused research into the coupling between tectonics and surface processes (Zeitler et al., 2001b; Finnegan et al., 2008; Korup et al., 2010; Koons et al., 2013; Wang et al., 2014). Both massifs show young (<10 Ma) high-grade metamorphism and partial melting (Burg et al., 1998; Zeitler et al., 2001a; Booth et al., 2009; Zeitler et al., 2014), extreme relief, and rapid erosion (Burbank et al., 1996;

Finnegan et al., 2008), expressed by exceptionally young thermochronologic ages (Stewart et al., 2008; Enkelmann et al., 2011; Bracciali et al., 2016; King et al., 2016). The two largest Himalayan rivers, the Indus and the Yarlung-Tsangpo-Siang-Brahmaputra, show hairpin bends and kilometer-scale steepened knick-zones as they cross these massifs (Fig. 1), sparking a debate on potential erosional controls on tectonics (Zeitler et al., 2001b; Finnegan et al., 2008; Seward and Burg, 2008; Wang et al., 2014; King et al., 2016).

Several models seek to explain these remarkable features. Purely tectonic mechanisms include range-parallel buckling in the indentor-plate corner (Burg et al., 1998), uplift driven by a geometrically stiffened bend in the subducting plate (Bendick and Ehlers, 2014), and orogen-parallel crustal transport arising from velocity/strain partitioning (Whipp et al., 2014). In contrast, the tectonic-aneurysm model (Zeitler et al., 2001a, 2001b; Koons et al., 2013) calls for coupling between river incision and rapid exhumation, leading to local crustal weakening and focusing rock pathways into the weakened, rapidly eroding zone. The inflowing material promotes topographic relief growth, localized exhumation and crustal weakening, creating a positive feedback loop between tectonics and surface processes.

Besides the mechanism, the timing of rapid exhumation is also controversial in the Namche Barwa massif. Early bedrock geochronology and thermochronology studies estimated the onset of rapid exhumation at ~4 Ma (Burg et al., 1998; Seward and Burg, 2008), whereas more recent data (Booth et al., 2009; Zeitler et al., 2014) suggested 8-10 Ma. Detrital thermochronology studies from the Brahmaputra Valley, the Surma Basin (Bangladesh), and the Bengal Fan have proposed rapid syntaxial exhumation starting at either 4-6 Ma (Najman et al., 2019) or <3 Ma (Chirouze et al., 2013; Bracciali et al., 2016). This inconsistency may arise from downstream modification and dilution of characteristic syntaxial exhumation signals (Bracciali et al., 2016; Gemignani et al., 2018); the most robust signal is therefore expected in proximal sedimentary records. Lang et al. (2016) modeled detrital thermochronology data from the proximal Siji section (Fig. 1) to infer an onset of rapid exhumation in Namche Barwa at 5-7 Ma.

To explore the exhumation history of the Namche Barwa syntaxis in more detail, we present new multisystem detrital thermochronology data from Neogene foreland-basin sandstone samples directly downstream of the syntaxis (Fig. 1) and interpret these using a thermo-kinematic inverse model.

NEW DETRITAL THERMOCHRONOLOGY DATA

We collected ten sandstone samples from three sedimentary sections close to the Siang-Brahmaputra confluence (Fig. 1). These sections are described by Govin et al. (2018), who also determined depositional ages ranging from 0.5 ± 0.3 Ma to 10.0 ± 2.0 Ma (see Table DR1 in the GSA Data Repository[1]). Provenance data indicate that the source region for these deposits included the Namche Barwa massif (Govin et al., 2018). Here we present new zircon fission-track (ZFT), muscovite $^{40}Ar/^{39}Ar$ (MAr) and rutile U-Pb (RUPb) data. Closure temperatures of these thermochronometers range from ~300 °C (ZFT) to >500 °C (RUPb), depending on grain size, composition and cooling rate (Reiners et al., 2018; Fig. DR5). As we target the signal from Namche Barwa, inferred to be the most rapidly exhuming part of the sediments' source area, we employ the minimum-age approach (Galbraith, 2005) to determine the youngest detrital age populations (see Data Repository for details). Sample preparation and analytical methods are reported in the Data Repository; single-grain ages are in Tables DR2-DR4 and Figures DR1-DR3. All ages are interpreted as cooling ages, as justified in the Data Repository.

A plot of the minimum ages of our samples together with literature data as a function of depositional age (Fig. 2), shows two distinct groups: for all three thermochronometers, samples with depositional ages >7.5 Ma have lag times (Bernet et al., 2001) that are >5 m.y., whereas samples with depositional ages ≤7 Ma show short lag times (around 2-3 m.y.). The latter group also shows several age inversions, where the system with lower closure temperature (ZFT) has minimum ages older than those for higher closure-temperature systems (MAr, RUPb). Such inversions are expected at high exhumation rates in some circumstances (Reiners et al., 2018); alternatively, some of these minimum ages may be unreliable for analytical reasons (i.e., poor counting statistics for grains with low daughter-product abundance; see discussion in the Data Repository). We discriminate between "internally consistent" samples, yielding ages ordered with respect to system closure temperatures within a sample and increasing monotonically with depositional age for the same system between samples, and inconsistent samples, which do not meet these criteria.

QUANTIFYING NAMCHE BARWA EXHUMATION

The slope of the lag-time trend indicates whether exhumation rates were steady, increasing, or decreasing through time (Bernet et al., 2001). We used a Bayesian approach (Glotzbach et al., 2011) to fit single- and multi-tier linear regressions to the lag times of internally consistent minimum ages (see Data Repository). The results (Fig. DR4) indicate increasing exhumation before ~7 Ma, followed by rapid steady exhumation between ~7 Ma and 0.5-2.0 Ma, and probable further acceleration since 0.5-2.0 Ma indicated by the youngest 2-3 samples. However, the onset of rapid exhumation will precede the arrival of young grains in the sedimentary record because of (a) the time required to exhume rocks from the thermochronologic closure depth to the surface, and (b) the time required to re-equilibrate the crustal thermal structure.

To better constrain the exhumation history, we used a 1-D version of the thermo-kinematic code *Pecube* (Braun et al., 2012) to predict a time-series of cooling ages resulting from step changes in exhumation rates, accounting for the effect of heat advection during exhumation. Comparison with the detrital thermochronology data is achieved through Neighborhood-Algorithm inversion; the model inverts for the exhumation rates and the timing of rate changes (Braun et al., 2012). Inversions use either the full dataset or only the internally consistent ages, and incorporate uncertainties in both minimum-peak ages and depositional ages. Two-stage and three-stage exhumation scenarios were tested. A full description of the procedure and the different inversions is provided in the Data Repository.

Our best-fit inversion uses the internally consistent dataset and implies a three-stage exhumation history for the Namche Barwa massif, with an early (8.2 ± 1.8 Ma) onset of rapid exhumation and a late (1.3 ± 0.8 Ma) acceleration (Fig. 3). Initial, intermediate, and final exhumation rates are 0.9 ± 0.4, 4.0 ± 2.0, and 8.6 ± 1.0 km/m.y., respectively. The onset of rapid exhumation at ~8 Ma is consistent with metamorphic Pressure-Temperature-time (PTt) paths from the Namche Barwa massif (Palin et al., 2015). Predicted exhumation rates agree with estimates from bedrock thermochronology (Seward and Burg, 2008; Zeitler et al., 2014; Bracciali et al., 2016), including those indicating a recent (< 1 Ma) acceleration (King et al., 2016). The total amount of exhumation since ~8 Ma predicted by our model is 42 ± 26 km; 1-4 times the ~15-20 km of exhumation since ~8 Ma inferred from PTt data (Fig. DR8).

DISCUSSION

Exhumation rates in Namche Barwa prior to ~8 Ma are comparable with those elsewhere in the Greater Himalaya during the Neogene (e.g., Thiede and Ehlers, 2013), suggesting similar tectonic processes. PTt data (Fig. DR8) suggest significant exhumation prior to ~8 Ma, captured by the initial phase of our model. In contrast, the clear evidence for accelerating exhumation at ~8 Ma and <2-3 m.y. lag times for all systems since that time, which we link to focused rapid exhumation in Namche Barwa, distinguish this easternmost detrital thermochronology record from those elsewhere in the Himalaya (e.g., Szulc et al., 2006; Chirouze et al., 2013). Our finding of sustained rapid exhumation since the late Miocene is consistent with previous work (Lang et al., 2016). However, inclusion of a high-temperature thermochronometer (RUPb) coupled with *Pecube* inversions allows us to reconstruct a more detailed three-stage exhumation history, reconciling previous apparently contrasting interpretations that emphasized either the earlier (~8 Ma; Booth et al., 2009; Zeitler et al., 2014) or later (<2 Ma; Wang et al., 2014; King et al., 2016) time of exhumation-rate change.

The onset of rapid exhumation at ~8 Ma is consistent with the scenario envisaged by Zeitler et al. (2014). The discrepancy between the amount of post ~8 Ma exhumation predicted by our data and that inferred from PTt data, for all but our lowest predicted exhumation rates, implies lateral inflow of mid-crustal material, consistent with the tectonic-aneurysm model (Zeitler et al., 2001a, 2001b; Koons et al., 2013). Thus, efficient coupling between crustal rock advection and surface erosion may have initiated at ~8 Ma, requiring the existence of a large through-going river system at that time. Whereas sedimentary provenance data record a drainage connection between the Yarlung-Tsangpo and the Brahmaputra since the early Miocene (~18 Ma; Lang and Huntington, 2014; Bracciali et al., 2015; Blum et al., 2018), it is unclear when the drainage pathway through the Namche Barwa massif via the Siang was established (Govin et al., 2018).

The trigger for rapid exhumation in Namche Barwa remains debated. It could have been initiated by indentor-corner dynamics (Burg et al., 1998; Bendick and Ehlers, 2014), with coupling between river incision and rapid exhumation developing subsequently, or it could have resulted from capture of the Yarlung-Tsangpo by the Siang shortly before ~8 Ma. The latter scenario is consistent with river-incision patterns upstream of Namche Barwa, which have been interpreted to record a wave of incision migrating upstream since ~10 Ma (Schmidt et al., 2015). However, that scenario requires prior Yarlung-Tsangpo drainage to the foreland via another, as yet unconstrained, pathway; a prediction that may be tested by provenance analysis of proximal foreland sediment records from candidate fossil trans-orogenic river systems.

Quaternary uplift of the Namche Barwa massif has been inferred from a thick wedge of post-2.6 Ma alluvium preserved immediately upstream (Wang et al., 2014; Fig. 4). This ponded sediment implies that rock uplift temporarily outpaced river incision, steepening the Siang river profile downstream. Quaternary capture of the Parlung river by the Yarlung-Tsangpo-Siang, as suggested by thermochronology (Seward and Burg, 2008; Zeitler et al., 2014) and provenance data (Lang and Huntington, 2014; Govin et al., 2018), would have increased erosional power in the gorge downstream of the capture point. In turn, this may have strengthened the feedback loop and triggered enhanced uplift and exhumation of Namche Barwa. River profiles provide insight into this possibility. The modern Yarlung-Tsangpo-Siang and Indus River profiles differ (Korup et al., 2010; Fig. 4), even though both flow through rapidly exhuming syntaxial massifs (Burbank et al., 1996; Zeitler et al., 2001b; Finnegan et al., 2008; Korup et al., 2010). The inferred pre-Quaternary profile of the Yarlung-Tsangpo-Siang resembles the modern Indus profile, with a more subdued knickzone across Namche Barwa and a morphologic plateau edge located farther upstream. Modeling of river incision (Koons et al., 2013) shows that the differences in modern river profiles can be induced by differing rock-uplift rates in the syntaxial massifs of ~5 and ~10 mm/yr (Fig. 4), consistent with the recent acceleration our data imply.

CONCLUSIONS

Our new data and modeling reveal a three-stage exhumation history for Namche Barwa, reconciling previous studies focusing on either an early or a late onset of rapid exhumation. Our results suggest that coupling between crustal rock advection and surface erosion initiated in the late Miocene and strengthened during the Quaternary. They suggest a potential role for river capture events in initiating and strengthening tectonic-erosion couplings in a tectonic aneurysm.

ACKNOWLEDGMENTS

This work is part of the Marie Curie Initial Training Network *iTECC* funded by the EU REA (grant agreement 316966). Rutile U-Pb analyses were funded by NERC through the NIGL facility (IP-1500-1114). CM is funded by Science Foundation Ireland (18/SIRG/5559). E. Enkelmann, K. Lang and P. Zeitler provided constructive reviews.

REFERENCES CITED

Bendick, R., and Ehlers, T.A., 2014, Extreme localized exhumation at syntaxes initiated by subduction geometry: Geophysical Research Letters, v. 41, no. 16, p. 5861–5867, doi: 10.1002/2014GL061026.

Bernet, M., Zattin, M., Garver, J.I., Brandon, M.T., and Vance, J.A., 2001, Steady-state exhumation of the European Alps: Geology, v. 29, no. 1, p. 35–38, doi: 10.1130/0091-7613(2001)029<0035:SSEOTE>2.0.CO;2.

Blum, M., Rogers, K., Gleason, J., Najman, Y., Cruz, J., and Fox, L., 2018, Allogenic and autogenic signals in the stratigraphic record of the deep-sea Bengal Fan: Scientific reports, v. 8, no. 1, p. 7–13, doi: 10.1038/s41598-018-25819-5.

Booth, A.L., Chamberlain, C.P., Kidd, W.S.F., and Zeitler, P.K., 2009, Constraints on the metamorphic evolution of the eastern Himalayan syntaxis from geochronologic and petrologic studies of Namche Barwa: Geological Society of America Bulletin, v. 121, no. 3-4, p. 385–407, doi: 10.1130/B26041.1.

Bracciali, L., Najman, Y., Parrish, R.R., Akhter, S.H., and Millar, I., 2015, The Brahmaputra tale of tectonics and erosion: Early Miocene river capture in the Eastern Himalaya: Earth and Planetary Science Letters, v. 415, no. C, p. 25–37, doi: 10.1016/j.epsl.2015.01.022.

Bracciali, L., Parrish, R.R., Najman, Y., Smye, A., Carter, A., and Wijbrans, J.R., 2016, Plio-Pleistocene exhumation of the eastern Himalayan syntaxis and its domal "pop-up": Earth Science Reviews, v. 160, p. 350–385, doi: 10.1016/j.earscirev.2016.07.010.

Braun, J., van der Beek, P., Valla, P., Robert, X., Herman, F., Glotzbach, C., Pedersen, V., Perry, C., Simon-Labric, T., and Prigent, C., 2012, Quantifying rates of landscape evolution and tectonic processes by thermochronology and numerical modeling of crustal heat transport using PECUBE: Tectonophysics, v. 524-525, no. C, p. 1–28, doi: 10.1016/j.tecto.2011.12.035.

Burbank, D.W., Leland, J., Fielding, E., and Anderson, R.S., 1996, Bedrock incision, rock uplift and threshold hillslopes in the northwestern Himalayas: Nature, v. 379, p. 505–510.

Burg, J.P., Nievergelt, P., Oberli, F., and Seward, D., 1998, The Namche Barwa syntaxis: evidence for exhumation related to compressional crustal folding: Journal of Asian Earth Sciences, v. 16, no. 2-3, p. 239–252, doi: 10.1016/S0743-9547(98)00002-6.

Chirouze, F., Huyghe, P., van der Beek, P., Chauvel, C., Chakraborty, T., Dupont-Nivet, G., and Bernet, M., 2013, Tectonics, exhumation, and drainage evolution of the eastern Himalaya since 13 Ma from detrital geochemistry and thermochronology, Kameng River Section, Arunachal Pradesh: Geological Society of America Bulletin, v. 125, no. 3-4, p. 523–538, doi: 10.1130/B30697.1.

Enkelmann, E., Ehlers, T.A., Zeitler, P.K., and Hallet, B., 2011, Denudation of the Namche Barwa antiform, eastern Himalaya: Earth and Planetary Science Letters, v. 307, no. 3-4, p. 323–333, doi: 10.1016/j.epsl.2011.05.004.

Finnegan, N.J., Hallet, B., Montgomery, D.R., Zeitler, P.K., Stone, J.O., Anders, A.M., and Yuping, L., 2008, Coupling of rock uplift and river incision in the Namche Barwa-Gyala Peri massif, Tibet: Geological Society of America Bulletin, v. 120, no. 1-2, p. 142–155, doi: 10.1130/B26224.1.

Galbraith, R.F., 2005, Statistics for Fission Track Analysis: Boca Raton, Fl, Chapman and Hall/CRC, 218 pp.

Gemignani, L., van der Beek, P.A., Braun, J., Najman, Y.M.R., Bernet, M., Garzanti, E., and Wijbrans, J.R., 2018, Downstream evolution of the thermochronologic age signal in the Brahmaputra catchment (eastern Himalaya): Implications for the detrital record of erosion: Earth and Planetary Science Letters, v. 499, p. 48–61, doi: 10.1016/j.epsl.2018.07.019.

Glotzbach, C., van der Beek, P.A., and Spiegel, C., 2011, Episodic exhumation and relief growth in the Mont Blanc massif, Western Alps from numerical modelling of thermochronology data: Earth and Planetary Science Letters, v. 304, no. 3-4, p. 417–430, doi: 10.1016/j.epsl.2011.02.020.

Govin, G., Najman, Y., Dupont-Nivet, G., Millar, I., van der Beek, P., Huyghe, P., O'Sullivan, P., Mark, C., and Vögeli, N., 2018, The tectonics and paleo-drainage of the easternmost Himalaya (Arunachal Pradesh, India) recorded in the Siwalik rocks of the foreland basin: American Journal of Science, v. 318, no. 7, p. 764–798, doi: 10.2475/07.2018.02.

King, G.E., Herman, F., and Guralnik, B., 2016, Northward migration of the eastern Himalayan syntaxis revealed by OSL thermochronometry: Science, v. 353, no. 6301, p. 800–804, doi: 10.1126/science.aaf2637.

Koons, P.O., Zeitler, P.K., and Hallet, B., 2013, Tectonic aneurysms and mountain building, *in* Shroder, J., and Owen, L.A., eds., Treatise on Geomorphology vol. 5, Tectonic Geomorphology: San Diego, CA, Academic Press, p. 318-349.

Korup, O., Montgomery, D.R., and Hewitt, K., 2010, Glacier and landslide feedbacks to topographic relief in the Himalayan syntaxes: Proceedings of the National Academy of Sciences, v. 107, no. 12, p. 5317–5322, doi: 10.1073/pnas.0907531107.

Lang, K.A., and Huntington, K.W., 2014, Antecedence of the Yarlung–Siang–Brahmaputra River, eastern Himalaya: Earth and Planetary Science Letters, v. 397, no. C, p. 145–158, doi: 10.1016/j.epsl.2014.04.026.

Lang, K.A., Huntington, K.W., Burmester, R., and Housen, B., 2016, Rapid exhumation of the eastern Himalayan syntaxis since the late Miocene: Geological Society of America Bulletin, v. 128, no. 9-10, p. 1403–1422, doi: 10.1130/B31419.1.

Najman, Y., Mark, C., Barfod, D.N., Carter, A., Parrish, R., Chew, D., and Gemignani, L., 2019, Spatial and temporal trends in exhumation of the Eastern Himalaya and syntaxis as determined from a multitechnique detrital thermochronological study of the Bengal Fan: Geological Society of America Bulletin, v. 131, no. 9-10, p. 1607–1622, doi: 10.1130/B35031.1.

Palin, R.M., Searle, M.P., St-Onge, M.R., Waters, D.J., Roberts, N.M.W., Horstwood, M.S.A., Parrish, R.R., and Weller, O.M., 2015, Two-stage cooling history of pelitic and semi-pelitic mylonite (sensu lato) from the Dongjiu-Milin shear zone, northwest flank of the eastern Himalayan syntaxis: Gondwana Research, v. 28, no. 2, p. 509–530, doi: 10.1016/j.gr.2014.07.009.

Reiners, P.W., Carlson, R.W., Renne, P.R., Cooper, K.M., Granger, D.E., McLean, N.M., and Schoene, B. (2018). Geochronology and Thermochronology: Chichester, UK, John Wiley & Sons, 445 pp., doi:10.1002/9781118455876.

Schmidt, J.L., Zeitler, P.K., Pazzaglia, F.J., Tremblay, M.M., Shuster, D.L., and Fox, M., 2015, Knickpoint evolution on the Yarlung river: Evidence for late Cenozoic uplift of the southeastern Tibetan plateau margin: Earth and Planetary Science Letters, v. 430, no. C, p. 448–457, doi: 10.1016/j.epsl.2015.08.041.

Seward, D., and Burg, J.-P., 2008, Growth of the Namche Barwa Syntaxis and associated evolution of the Tsangpo Gorge: Constraints from structural and thermochronological data: Tectonophysics, v. 451, no. 1-4, p. 282–289, doi: 10.1016/j.tecto.2007.11.057.

Stewart, R.J., Hallet, B., Zeitler, P.K., Malloy, M.A., Allen, C.M., and Trippett, D., 2008, Brahmaputra sediment flux dominated by highly localized rapid erosion from the easternmost Himalaya: Geology, v. 36, no. 9, p. 711–39, doi: 10.1130/G24890A.1.

Szulc, A.G., Najman, Y.M.R., Sinclair, H.D., Pringle, M., Bickle, M., Chapman, H., Garzanti, E., Andò, S., Huyghe, P., Mugnier, J.L., Ojha, T., and DeCelles, P., 2006, Tectonic evolution of the Himalaya constrained by detrital ^{40}Ar-^{39}Ar, Sm-Nd and petrographic data from the Siwalik foreland basin succession, SW Nepal: Basin Research, v. 18, no. 4, p. 375–391, doi: 10.1111/j.1365-2117.2006.00307.x.

Thiede, R.C., and Ehlers, T.A., 2013, Large spatial and temporal variations in Himalayan denudation: Earth and Planetary Science Letters, v. 371-372, no. C, p. 278–293, doi: 10.1016/j.epsl.2013.03.004.

Wang, P., Scherler, D., Liu-Zeng, J., Mey, J., and Avouac, J.P., 2014, Tectonic control of Yarlung Tsangpo Gorge revealed by a buried canyon in Southern Tibet: Science, v. 346, no. 6212, p. 978–981, doi: 10.1126/science.1259041.

Whipp, D.M., Beaumont, C., and Braun, J., 2014, Feeding the “aneurysm”: Orogen - parallel mass transport into Nanga Parbat and the western Himalayan syntaxis: Journal of Geophysical Research: Solid Earth, v. 119, p. 5077–5096, doi: 10.1002/ 2013JB010929.

Zeitler, P.K., Koons, P.O., Bishop, M.P., Chamberlain, C.P., Craw, D., Edwards, M.A., Hamidulah, S., Qasim Jan, M., Khan, M.A., Khattak, M.U.K., Kidd, W.S.F., Lackie, R.L., Meltzer, A.S., Park, S.K., et al., 2001a, Crustal reworking at Nanga Parbat, Pakistan: Metamorphic consequences of thermal-mechanical coupling facilitated by erosion: Tectonics, v. 20, no. 5, p. 712–728.

Zeitler, P.K., Meltzer, A.S., Brown, L., Kidd, W.S.F., Lim, C., and Enkelmann, E., 2014, Tectonics and topographic evolution of Namche Barwa and the easternmost Lhasa block, Tibet: Geological Society of America Special Paper, v. 507, p. 23–58, doi: 10.1130/2014.2507(02).

Zeitler, P.K., Meltzer, A.S., Koons, P.O., Craw, D., Hallet, B., Chamberlain, C.P., Kidd, W.S.F., Park, S.K., Seeber, L., Bishop, M.P., and Shroder, J.F., 2001b, Erosion, Himalayan geodynamics, and the geomorphology of metamorphism: GSA Today, v. 11, no. 1, p. 4–9.

FIGURE CAPTIONS

Figure 1. A: Topography, active faults (white) and major rivers (blue) of the Himalaya. Triangles show syntaxial massifs: NP – Nanga Parbat; NB – Namche Barwa. Box shows location of B. B: Eastern syntaxis, showing the Namche Barwa massif, Yarlung-Tsangpo-Siang-Brahmaputra River and sampling locations. Stars indicate the sampled sections; black lines show major faults. Orange and purple dashed lines are contours of zircon fission-track/zircon (U-Th)/He (ZFT/ZHe) and biotite ^{40}Ar/^{39}Ar cooling ages <2 Ma, respectively (Gemignani et al., 2018). NB: Namche Barwa; GP: Gyala Peri; *IYSZ*: Indus-Yarlung Suture Zone; *NLT*: Nam La Thrust.

Figure 2. Minimum peak ages for new and published data, as a function of depositional age. Selected lag-time contours (in m.y.) are shown as black lines. Data in lighter shade are internally inconsistent and not used in preferred modeling runs. ZFT: zircon fission track; MAr: Muscovite ^{40}Ar/^{39}Ar; RUPb: Rutile U-Pb. Sample numbers (Table DR1) indicate section (REM: Remi; SG: Siang). Lang et al. (2016) samples are from the Siji section. Modern river-sand data are from Stewart et al. (2008), Enkelmann et al. (2011) (ZFT); Bracciali et al. (2016) (ZFT, RUPb); Lang et al. (2016), Gemignani et al. (2018) (MAr).

Figure 3. Result of preferred three-stage thermo-kinematic model inversion. A-C: individual forward-model results (dots colored according to misfit) and posterior probability-density

functions (pdf's) of the parameter values; A: initial exhumation rate versus intermediate exhumation rate; B: final exhumation rate versus intermediate exhumation rate; C: onset time versus acceleration time. Crosses in scatterplots and thick lines in pdf's indicate most likely parameter values, indicated next to pdf with 1σ uncertainty; stars indicate best-fit model parameters (in parentheses next to pdf). D: fit of the best-fit model (colored lines; orange: ZFT; purple: MAr; blue: RUPb) to the data (colored symbols with error bars).

Figure 4. Indus and Yarlung-Tsangpo-Siang River profiles. Zones of rapid uplift and exhumation in the Nanga Parbat-Haramosh (*NPHM*) and Namche Barwa (*NBM*) massifs are shown as grey boxes with bounding faults (*F.*) in black. The edge of the morphologic Tibetan plateau is indicated with a vertical arrow. The thickness of Quaternary alluvial sediments (yellow) upstream of Namche Barwa is from Wang et al. (2014); inferred pre-Quaternary profile indicated with dashed line. Inset (modified from Koons et al., 2013) shows modeled river profile (solid line) and rock uplift (dashed) after 0.5 m.y. for a river incising a 3-km high plateau bounded by a zone of anticlinal uplift (grey), for maximum uplift rates of 0 (black), 5 (blue) and 11 (red) mm/yr. Arrows indicate morphologic edge of plateau.

[1]GSA Data Repository item 202Xxxx, Methods descriptions, analytical data and inversion results, is available online at www.geosociety.org/pubs/ft20XX.htm, or on request from editing@geosociety.org.

Figure 1

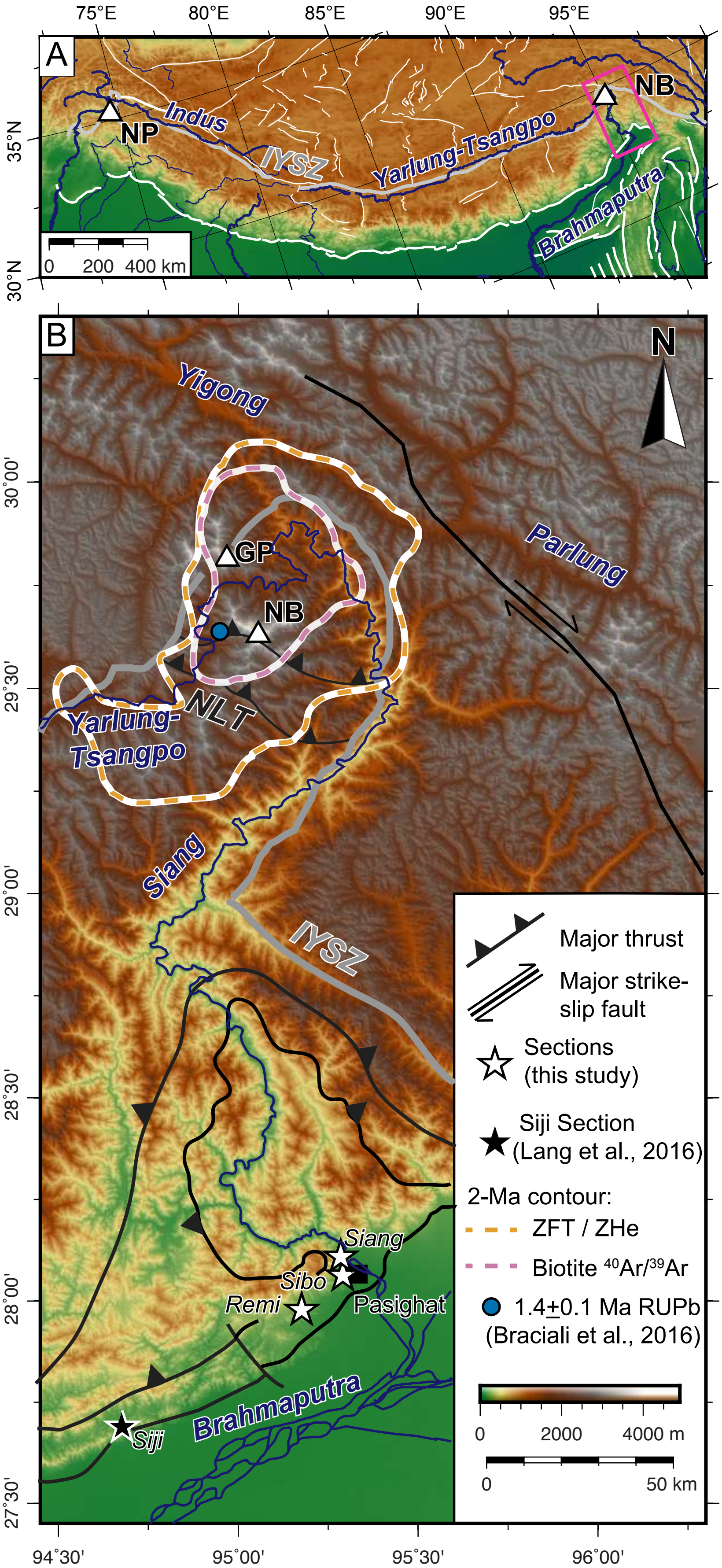

75°E
80°E
85°E
90°E
95°E
35°N
30°N
A
NP
Indus
IYSZ
Yarlung-Tsangpo
NB
Brahmaputra
0 200 400 km
B
N
Yigong
Parlung
GP
NB
NLT
Yarlung-Tsangpo
Siang
IYSZ
Siang
Sibo
Remi
Pasighat
Siji
Brahmaputra
30°00'
29°30'
29°00'
28°30'
28°00'
27°30'
94°30'
95°00'
95°30'
96°00'
Major thrust
Major strike-slip fault
Sections (this study)
Siji Section (Lang et al., 2016)
2-Ma contour:
ZFT / ZHe
Biotite 40Ar/39Ar
1.4±0.1 Ma RUPb (Braciali et al., 2016)
0
2000
4000 m
0
50 km

Figure 2

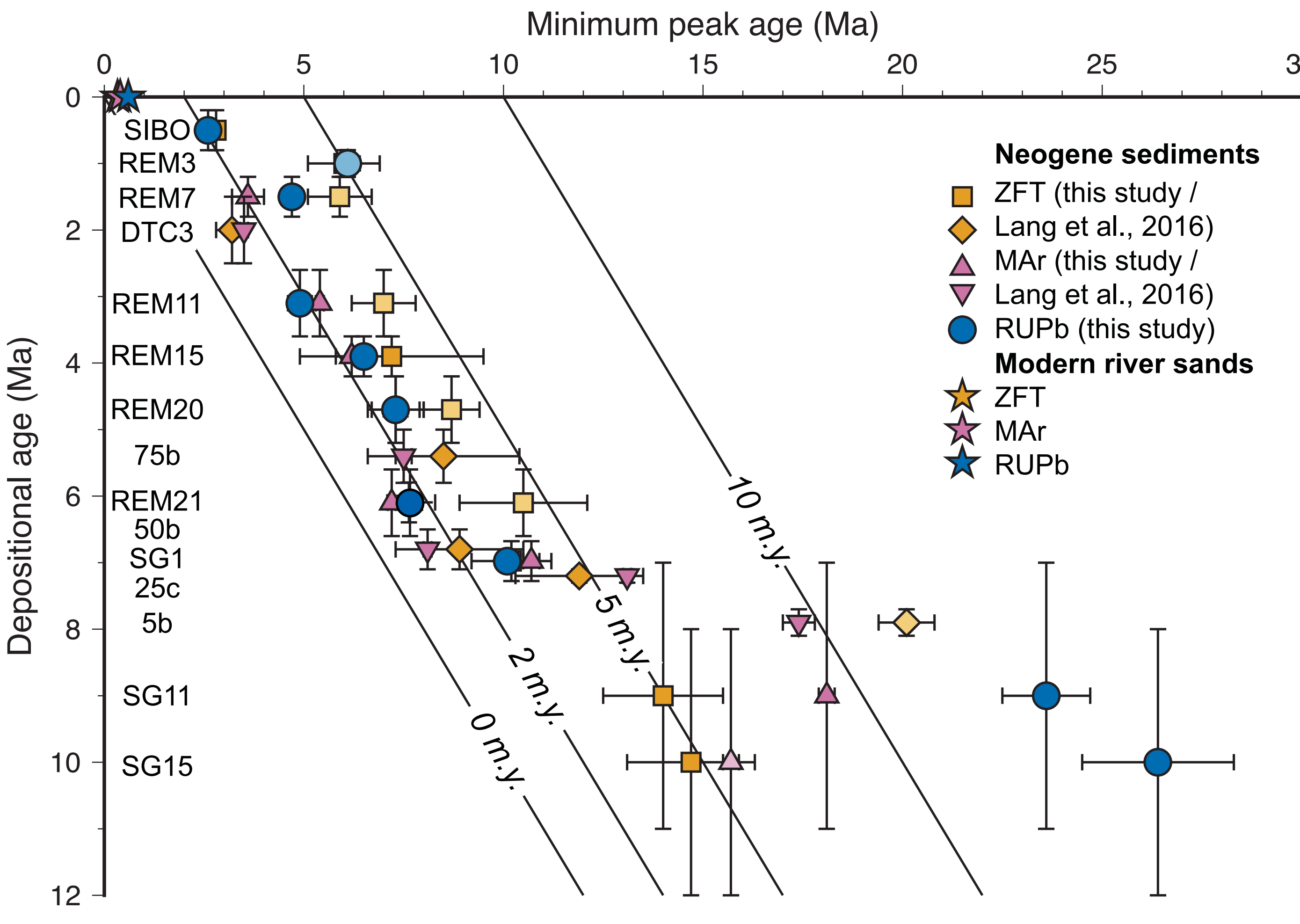

Minimum peak age (Ma)
0
5
10
15
20
25
30
Depositional age (Ma)
0
2
4
6
8
10
12
SIBO
REM3
REM7
DTC3
REM11
REM15
REM20
75b
REM21
50b
SG1
25c
5b
SG11
SG15
0 m.y.
2 m.y.
5 m.y.
10 m.y.
Neogene sediments
ZFT (this study /
Lang et al., 2016)
MAr (this study /
Lang et al., 2016)
RUPb (this study)
Modern river sands
ZFT
MAr
RUPb

Figure 3

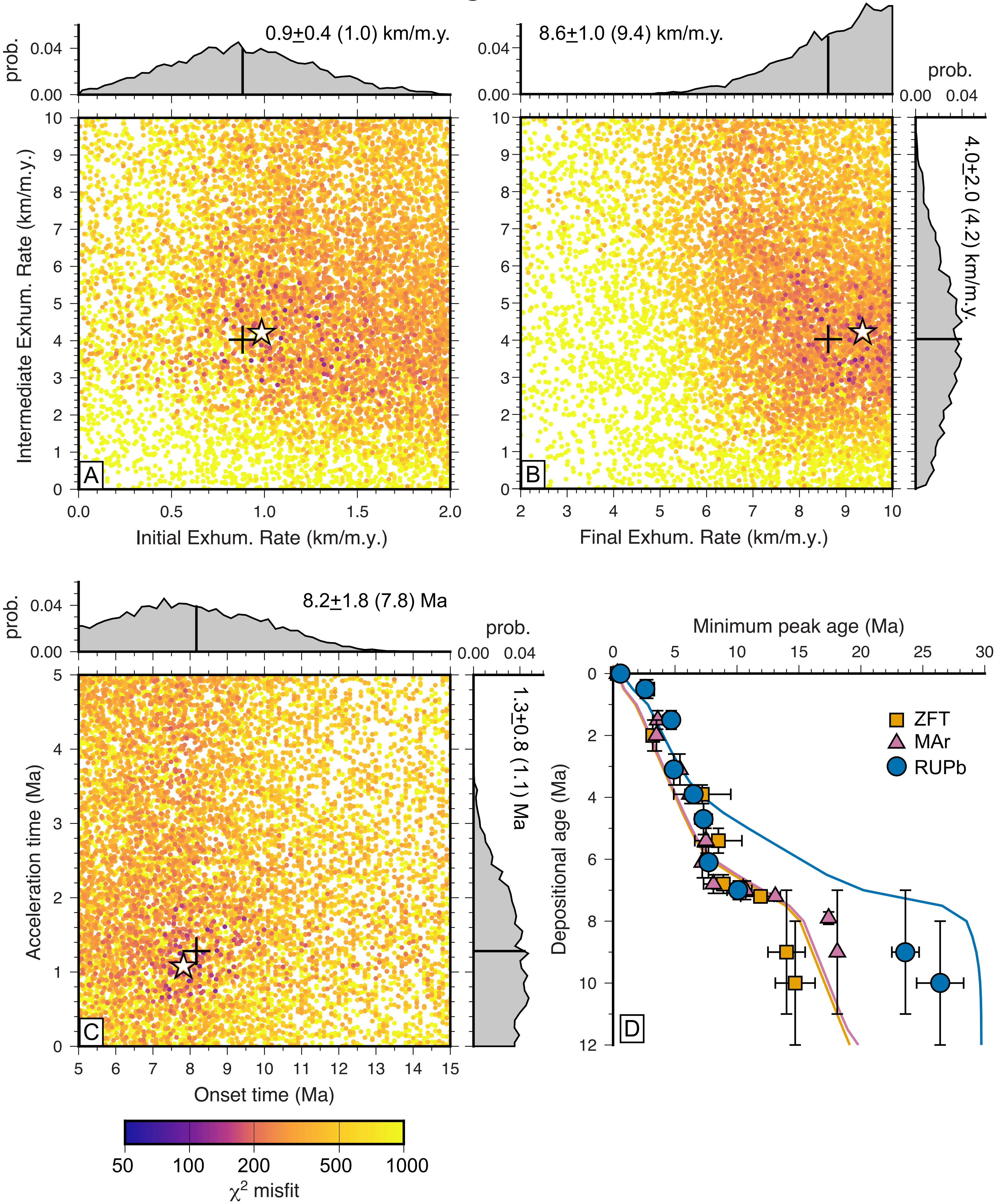

prob.
0.9±0.4 (1.0) km/m.y.
8.6±1.0 (9.4) km/m.y.
4.0±2.0 (4.2) km/m.y.
Intermediate Exhum. Rate (km/m.y.)
Initial Exhum. Rate (km/m.y.)
Final Exhum. Rate (km/m.y.)
A
B
8.2±1.8 (7.8) Ma
1.3±0.8 (1.1) Ma
Acceleration time (Ma)
Onset time (Ma)
C
Minimum peak age (Ma)
Depositional age (Ma)
ZFT
MAr
RUPb
D
χ^2 misfit

Figure 4

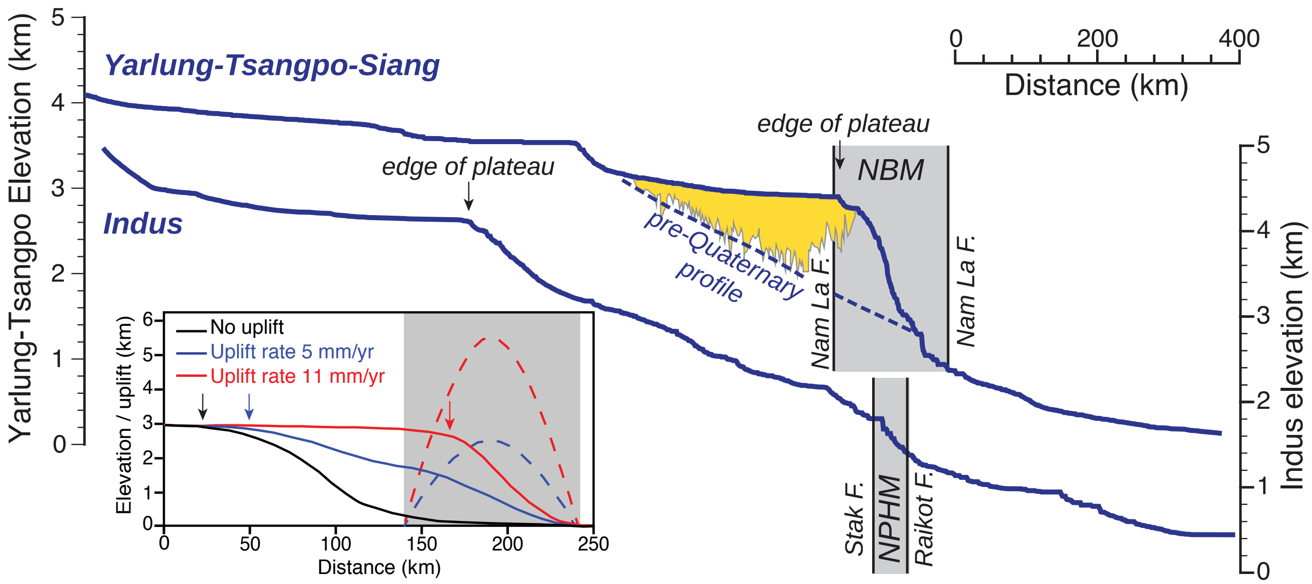

Yarlung-Tsangpo-Siang
Indus
Yarlung-Tsangpo Elevation (km)
Indus elevation (km)
Distance (km)
edge of plateau
edge of plateau
NBM
pre-Quaternary profile
Nam La F.
Nam La F.
Stak F.
NPHM
Raikot F.
No uplift
Uplift rate 5 mm/yr
Uplift rate 11 mm/yr
Elevation / uplift (km)
Distance (km)